Colloids and Surfaces B: Biointerfaces 91 (2012) 26–33

Contents lists available at SciVerse ScienceDirect

Colloids and Surfaces B: Biointerfaces

journal homepage: www.elsevier.com/locate/colsurfb

Coordination forces between lipid bilayers produced by ferricyanide and Ca^{2+}

María A. Frías[a], Griselda Contis[b], Axel Hollmann[a], E. Anibal Disalvo[a,*]

[a] Laboratory of Physical-Chemistry of Lipid Membranes, School of Pharmacy and Biochemistry, Junín 956, University of Buenos Aires, Buenos Aires, Argentina
[b] School of Odonthology, University of Rosario, Rosario, Argentina

ARTICLE INFO

Article history:
Received 15 September 2011
Accepted 17 October 2011
Available online 3 November 2011

Keywords:
Lipid membranes
Ferricyanide
Ca^{2+} ions
Vesicle aggregation
Complex adsorption
Zeta potential

ABSTRACT

Attractive forces usually invoked to take place in membrane–membrane contact in aggregation are hydrogen bonding cross-linkings and hydrophobic interactions between opposing surfaces. However, little is known in relation to the presence of coordination forces in the membrane–membrane interaction. These are understood as those that may be favoured by the formation or the participation of coordination complexes between surface specific groups. In this work, we have analyzed the formation of this type of aggregates between phosphatidylcholine vesicles mediated by a coadsorption of ferricyanide and Ca^{2+} ions to the interface. The results obtained by surface potential measures, optical and electronic microscopy, FTIR and ^1H NMR spectroscopies indicate that ferricyanide $[Fe(CN)_6]^{3-}$ but not of ferrocyanide $[Fe(CN)_6]^{4-}$ can form the complex when Ca^{2+} has been adsorbed previously to the membrane surface. In this condition, the anion is likely to act as a bridge between two opposing membranes causing a tight aggregation in which geometry and the polarizability of the ligands to Fe^{3+} play a role.

1. Introduction

Forces at the surface of a membrane control the ordering and the packing of adsorbing molecules in a two dimensional arrangement. In addition, intermolecular repulsion and attractive forces have been postulated to take place in the interplanar membrane–membrane contact in aggregation and fusion [1].

Repulsions hindering the membrane–membrane contact are identified with charge repulsion and non electrostatic forces including hydration (dipole potential), undulations and steric forces [2,3]. The attractive forces usually invoked are hydrogen bonding crosslinkings and hydrophobic interactions between opposing non polar surfaces.

The role of electrostatic forces in the interactive process is mainly ascribed to the screening of the surface charge repulsion, not to a net attractive force [4]. Electrostatic repulsions are drastically reduced by the high ionic strength at physiological salt concentrations. Thus, the reduction of this repulsion is relevant in the way that it makes possible the interaction between surfaces via short range attractive forces, such as van der Waals and H bonds.

One exception to this rule seems to be Ca^{2+} and others high density charge ions (high charge to radius ratio) ions, such as La^{3+}, that strongly bind to phosphate groups of zwitterionic and negative phospholipids causing changes in packing and polymorphic arrangements of lipid molecules [5]. Calcium ions bind naturally to negatively charged phospholipids as phosphatidylserine [6], phosphatidylinositol [7] and phosphatidylglycerol [8] but rather weakly to zwitterionic lipids as phosphatidylcholine (PC) and phosphatidylethanolamines (PE) [9–11]. However, Ca^{2+} affects the band absorption of asymmetric and symmetric phosphate stretching modes as measured by the FTIR spectra, which has been ascribed to the dehydration caused by the interaction [11–13].

The binding constants of Ca^{2+} ions to pure PC bilayers may differ from those corresponding to mixtures of PC with another kind of phospholipids, e.g., phosphatidylglycerol (PG) [14]. In general, the stoichiometry of the Ca^{2+}/PC binding is 1:1 in the fluid state and 1:2 in the gel state [15]. In chemically synthesized phospholipids like dipalmitoylphosphatidylcholine (DPPC) different changes in the state of assembly at their phase transition temperatures have been reported [16]. Faure et al. [16] found that the tilt angle of DPPC molecules was 30° in the gel phase and 0° in the fluid phase while the geometrical parameters of the head group remained constant throughout the different phases [16].

Among the techniques to detect Ca^{2+} adsorption on suspended particles, measure of the zeta potential of PC liposomes in ionic solutions is a direct one [10,17]. With this technique also anion adsorption can be detected.

Anions may also adsorb to the lipid membrane due to the increased polarizability of their electronic clouds following the Hoffmeister series [18–20]. In this case, the surface acquires a negative surface charge density. Ferricyanide is not included in the Hoffmeisster series [20]. However, due to the presence of CN^- ligands, ferricyanide and ferrocyanide anions should be in the end

* Corresponding author.
E-mail address: eadisal@yahoo.com.ar (E.A. Disalvo).

0927-7765/$ – see front matter © 2011 Elsevier B.V. All rights reserved.
doi:10.1016/j.colsurfb.2011.10.046

near ClO_4^-. The corresponding radii are 400 and 450 pm according to Marcus while Ca^{2+} is 100 pm [21].

The titration of sonicated vesicles of egg phosphatidylcholine with $[Fe(CN)_6]^{3-}$ in the presence of Ca^{2+} results in the formation of aggregates [22]. The turbidity increase caused by these aggregates cannot be reversed by EDTA treatment. In addition, no rearrangement of the bilayer structure has been found in this process. This was deduced from the absence of leakage of a dye trapped in sonicated vesicles parallel to a turbidity increase [22]. The aggregation seems to be dependent on the Ca^{2+} content of the vesicles, the outer Ca^{2+}, the $[Fe(CN)_6]^{3-}$ concentration and the order of addition of Ca^{2+} and $[Fe(CN)_6]^{3-}$. The results were explained by a specific adsorption of $[Fe(CN)_6]^{3-}$ to bilayers of sonicated vesicles, in contrast to other anions of a similar radius but with a higher charge such as ferrocyanide $[Fe(CN)_6]^{4-}$ that were unable to produce aggregation in the presence of Ca^{2+}. This was indicative that the charge is not a determinant property in the aggregation phenomena.

In order to have an insight on the forces and structural arrangements, conveying to the formation of aggregates as a function of the nature of the complex, the aim of this article is to study the binding of $[Fe(CN)_6]^{3-}$ and Ca^{2+} to dipalmitoylphosphatidylcholine (DPPC) layers in the fluid and gel states by electrophoretic mobility, light scattering measurements FTIR and ^1H NMR spectroscopies. Optical and electronic microscopy provided a direct visualization of organization, or lack thereof, and can thus provide critical information about the mechanisms of aggregation.

A model of the interlamellar structure is proposed on the base of these results.

2. Materials and methods

2.1. Lipids and chemicals

Egg phosphatidylcholine (eggPC) and dipalmitoylphosphatidylcholine (DPPC) were obtained from Avanti Polar Lipids Inc. (Alabaster, AL). The purity of the lipids was checked by running the FTIR spectra of lyophilized samples and by differential scanning calorimetry (DSC) and by thin layer chromatography (TLC), using the solvent mixture corresponding to each type of phospholipid. Single spots after exposure to the suitable developers were obtained. Peroxidation levels in unsaturated phospholipids (eggPC) were checked by ultraviolet spectroscopy, and it was found negligible under the conditions employed.

Calcium chloride ($CaCl_2$) was obtained from Sigma Aldrich Chemical Co. Inc. (St. Louis, MO) and $[Fe(CN)_6]^{-3}$ from Analytical reagent – Mallinckrodt.

All other chemicals were of analytical grade and ultrapure water (conductivity 0.09 μS/cm, pH 6 ± 0.3) was obtained in an Osmoion equipment (Apema, Buenos Aires, Argentina).

$K_3[Fe(CN)_6]$ and $CaCl_2$ stock solutions of a concentration 10 and 8 mM, respectively were prepared in tridistilled water and used as a blank.

2.2. Light scattering measurements

Lipids in chloroform solution were dried to form a film under a stream of nitrogen. Then, they were rehydrated in solutions of $K_3[Fe(CN)_6]$ and $CaCl_2$ heating above the transition temperature with gently agitation during 15 min to produce multilamellar vesicles (MLV's) [23]. Large unilamellar vesicles (LUV) of DPPC were prepared by extrusion of MLV's through Nuclepore® membranes of 400 nm pore diameter using an Avanti Mini-Extruder.

In all cases, the relation lipid to water was maintained in order to make the preparation more reproducible.

In order to investigate aggregation effects, turbidity changes were followed by adding known amounts of $K_3[Fe(CN)_6]$ and $CaCl_2$ to LUV's DPPC dispersions.

The turbidity changes at 25 °C were followed by measuring the changes in the absorbance at 450 nm in a Hitachi U-2000 spectrophotometer by adding known amounts of the stock $K_3[Fe(CN)_6]$ and $CaCl_2$ solutions to a measured volume of water or LUV's DPPC vesicles.

2.3. Optical microscopy

Morphological evaluation of LUV's and multilamellar liposomes with the addition of 10 mM $[Fe(CN)_6]^{-3}$ and/or 8 mM $CaCl_2$, prepared as were described below was conducted using an inverted microscope CKX41 (Olympus, Japan), and were visualized by digital Olympus QColor3-RTV-R (Olympus). Finally images were analyzed by software Q-Capture Pro (Q-imaging, Surrey, BC Canada).

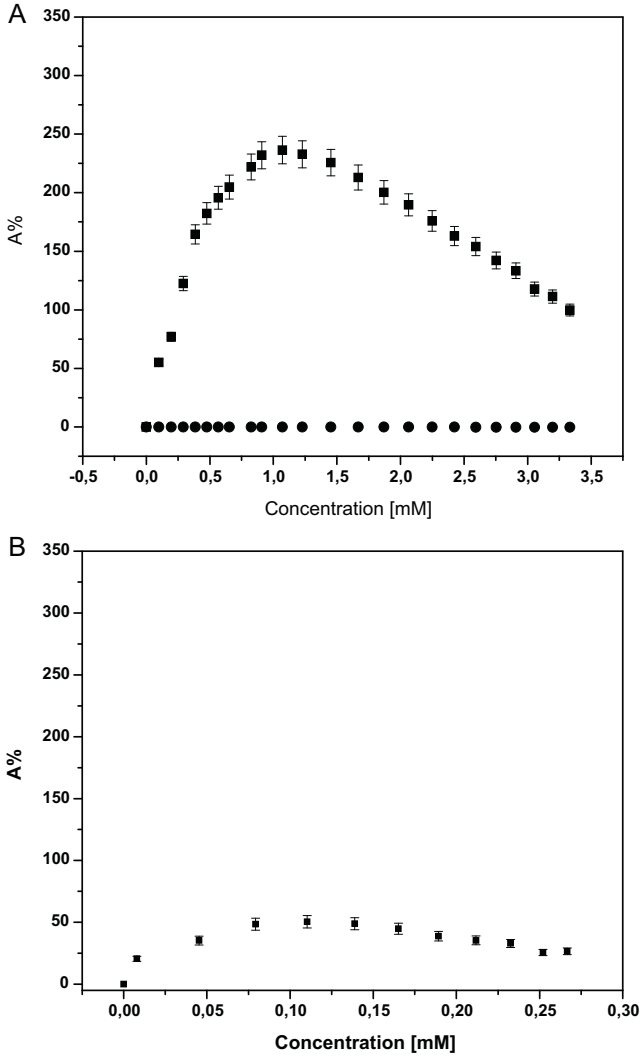

Fig. 1. Aggregation of LUV's induced by $[Fe(CN)_6]^{3-}$ and Ca^{2+}. (A) Turbidity changes induced by $[Fe(CN)_6]^{3-}$ on (●) LUV's DPPC vesicles without Ca^{2+} in the suspension media and, in the presence of 8 mM Ca^{+2} (■). (B) Turbidity changes of LUV's DPPC vesicles titrated with an equimolar solution of Ca^{+2} and $[Fe(CN)_6]^{3-}$·(Ca^{2+}/$[Fe(CN)_6]^{3-}$ ratio = 0.8).

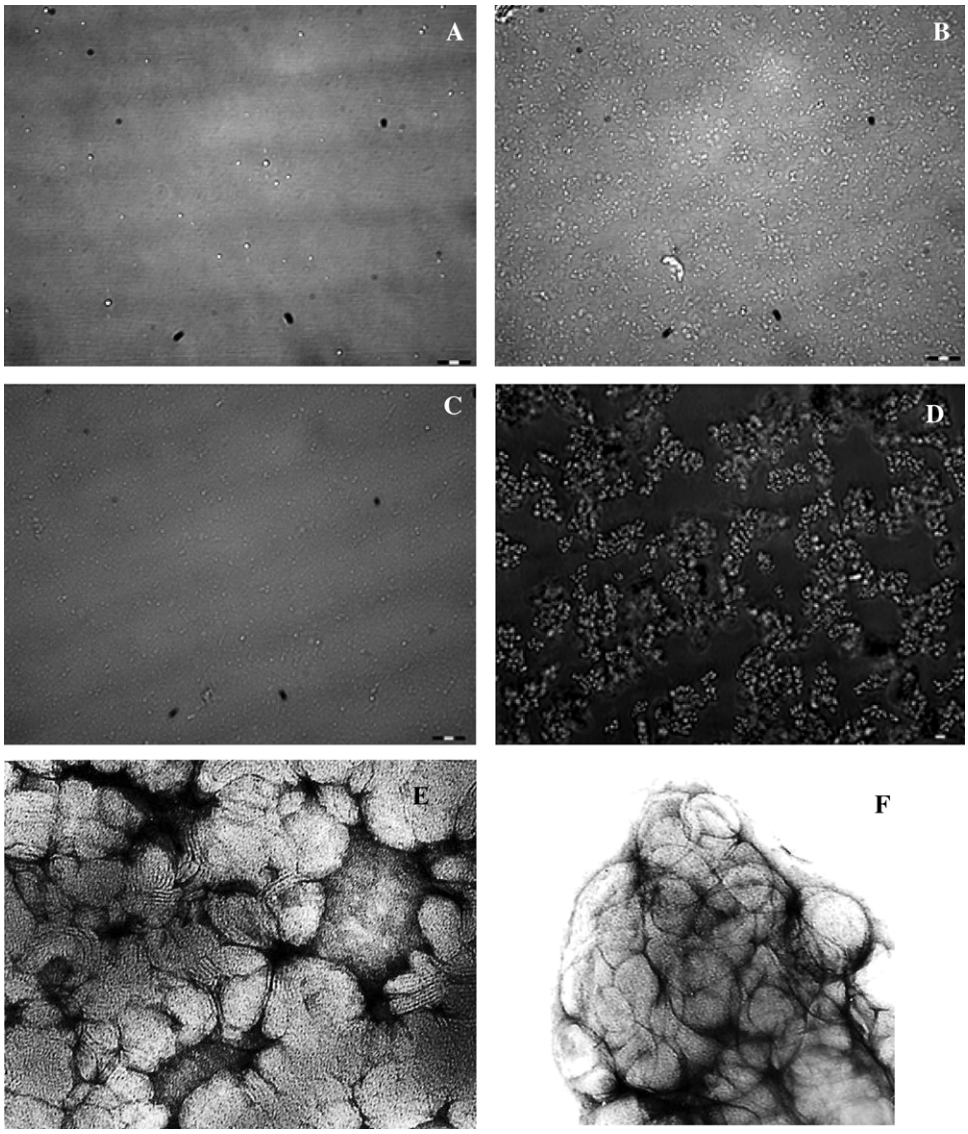

Fig. 2. Microscopic visualization of vesicle aggregation. LUV's DPPC vesicles dispersed in water (A); in 10 mM $[Fe(CN)_6]^{3-}$; (B) in 8 mM Ca^{2+} (C); and in $[Fe(CN)_6]^{3-}$ in presence of 8 mM Ca^{2+} (D). All pictures were obtained after 30 min of incubation under agitation. Bar: 20 μm. (E) Partial visualization of aggregates by electronic microscopy formed in the presence of Ca^{2+} and $[Fe(CN)_6]^{3-}$, (F) same as E after the incubation in ascorbic acid.

2.4. Electronic microscopy

Small drops of each sample were located on a 400 mesh EM carbon film grid. The preparation was let dry at 22 °C for 15–20 s. Then, two drops of uranyl acetate 1%, pH 7.2 were added. The sample was dried out in moisture condition in Petri dish for 10–15 min. Negative stained grids were examined in a JEM-1200 electron microscope at magnification of 15,000 and 75,000×.

2.5. Zeta potential in liposomes

The zeta potential (ζ) of MLV's liposomes of lipids in the fluid state at different calcium chloride concentrations was determined in Zeta-Meter System 3.0 equipment (Staunton, VA, USA) at 22 °C.

The electrophoretic mobility (μ) of multilamellar liposomes was determined in a capillary cell in which two electrodes were connected to a direct current source. The total lipid concentration in all cases was 46 μM.

Data reported are the average of the measurements done, for each condition, with, at least, three different batches of liposomes. A total of 20 measurements were done for the different batches.

The zeta potential (ζ) was calculated from the mobility using the Helmholtz–Smoluchowski equation:

$$\xi = \frac{\mu\eta}{\varepsilon\varepsilon_o}$$

where, ε and ε_o are the dielectric permittivity of the aqueous solution and the permittivity of the free space; η is the dynamic viscosity of the suspension.

2.6. ATR-FTIR spectroscopy

An ATR-FTIR spectrometer (Thermo Nicolet 380) with a DTGS temperature-stabilized coated detector was used (4000–400 cm^{-1}). This was equipped with an attenuated total reflection Zinc Selenide (ZnSe) crystal accessory (ATR).

The resolution of the equipment employed was 2 cm^{-1}. A total of 64 scans were done in each condition and the spectra were analyzed using the mathematical software provided by the instrument. A number of different samples were processed in order to obtain

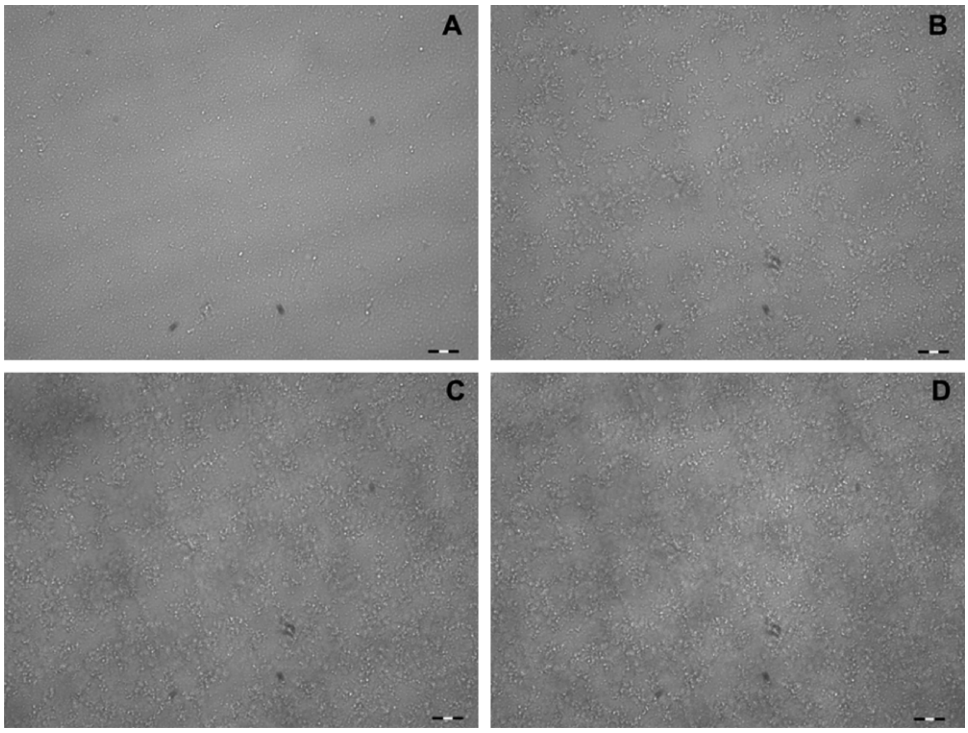

Fig. 3. Time sequence of aggregation after the addition of $Ca^{2+}/[Fe(CN)_6]^{3-}$ ratio. Optical microscopy visualization of DPPC LUV dispersions immediately after addition of $[Fe(CN)_6]^{3-}$ in the presence of 8 mM Ca^{2+} (A), and incubated 30 min (B), 60 min (C) and 90 min (D). Bar: 20 μm.

a standard deviation below the resolution of the equipment. The spectra were analyzed using Omnic v 7.3 and processed with Origin v 7.5.

2.7. ^1H NMR measurements

^1H NMR measurements were performed in a Bruker AC-250 MHz instrument with sample spinning at 298 K. A simple normal spectrum was gathered and peak positions were internally referenced to the residual peak at 4.63 ppm. Observations of the effect of the ions were made on the choline peak centered at 3.1 ppm.

3. Results

A turbidity increase is noticed when vesicles are titrated with $[Fe(CN)_6]^{3-}$ in the presence of Ca^{2+} (Fig. 1A). In the same figure, it is observed that no effect on turbidity is found when $[Fe(CN)_6]^{3-}$ is added to liposomes in the absence of Ca^{2+} ions.

The titration of large unilamellar vesicles in the presence of 8 mM Ca^{2+} show a maximum at 1 mM $[Fe(CN)_6]^{3-}$ (upper curve), showing that the effectiveness of the aggregation decreases in an excess of $[Fe(CN)_6]^{3-}$ for the initial Ca^{2+} relation.

In this direction, the titration of similar concentration of vesicles with an equimolar solution of Ca^{+2} and $[Fe(CN)_6]^{3-}$ show an increase in turbidity reaching a plateau at 0.08 mM (Fig. 1B).

The turbidity increase corresponds to the formation of aggregates as visualized by optical and electronic microscopies (Fig. 2). LUV's DPPC dispersions in water (A), in 10 mM $[Fe(CN)_6]^{3-}$ (B) and in 8 mM Ca^{2+} (C) are clearly separated. In contrast, Fig. 2D denotes that vesicles are aggregated in clusters of 15.9 ± 4.32 μm. Details of the vesicle membrane surfaces obtained by transmission electron microscopy are shown in Fig. 2E, in which an undulated rough surface is noticeable when the aggregates are formed. This roughness disappears when the ferricyanide is reduced to ferrocyanide by the addition of ascorbic acid (Fig. 2F).

The appearance of these aggregates corresponds to the turbidity changes of Fig. 1A and B produced by the simultaneous presence of Ca^{2+} and $[Fe(CN)_6]^{3-}$ in the lipid dispersions after 30 min of incubation under agitation. The sequence of vesicle aggregation at different times after the addition of Ca^{2+} and $[Fe(CN)_6]^{3-}$ is shown in Fig. 3.

To understand the mechanism of aggregation in terms of the surface properties conferred by ferricyanide and Ca^{2+}, we studied the adsorption of Ca^{2+} and ferricyanide ions to vesicles at low lipid concentrations in which aggregation does not occur. To find the appropriate conditions for adsorption studies by this technique, we determined the profile of turbidity by the addition of PC MLV's to a solution containing 8 mM Ca^{2+} and 10 mM $[Fe(CN)_6]^{3-}$. A continuous increase in turbidity as a consequence of the increase in the concentration of dispersed particles was followed by a sudden increase in turbidity at 0.3 mM lipids which reaches a stationary value at higher concentrations (Fig. 4). The tightly bound aggregates observed in Fig. 2D by optical microscopy were found above that critical lipid concentration.

Below 0.3 mM, aggregates are not observed, and the surface potential (zeta potential), measured by electrophoretic mobility, is around −20 and −25 mV with subsequent additions of $[Fe(CN)_6]^{3-}$ to vesicles without Ca^{2+} (Fig. 5A, lower curve). In contrast, in the same figure (upper curve) a sharp shift towards positive potentials is observed when liposomes are titrated with Ca^{2+}. At 7–8 mM Ca^{2+} the surface potential value is around 0 mV.

In this condition, i.e. when the vesicle's potential has been zeroed by calcium, the addition of $[Fe(CN)_6]^{3-}$ promotes a pronounced displacement of the potential to negative values (Fig. 5B upper curve). The same final value of zeta potential is obtained when Ca^{2+} is added to the dispersion in the presence of $[Fe(CN)_6]^{3-}$ (Fig. 5B, lower curve). This denotes that independently of the sequence of addition the same final surface state is produced.

The ^1H NMR measurements denote that the choline groups are not perturbed in the conditions at which aggregation is not produced, i.e. when Ca^{2+} or $[Fe(CN)_6]^{3-}$ are added in separated batches

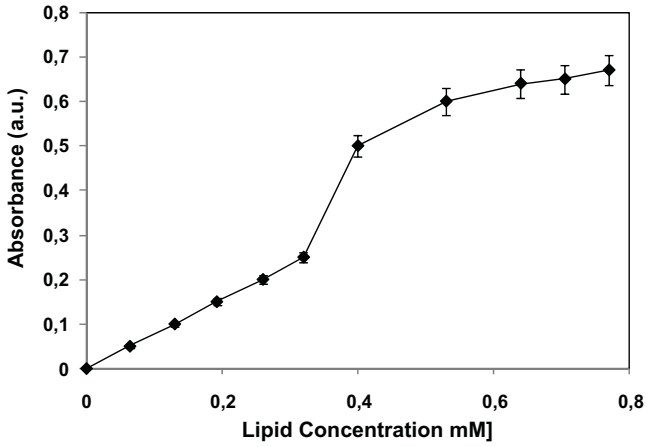

Fig. 4. Critical point in the aggregation of pc liposomes, in the presence of Ca^{2+} and $[Fe(CN)_6]^{3-}$, as measured by the increase in the turbidity of the sample as a function of added lipids.

of lipids. This corresponds to the points at zero concentration in Fig. 5B (vesicles in Ca^{2+} upper curve; vesicles in $[Fe(CN)_6]^{3-}$, lower curve). However, the simultaneous presence of both ionic species promotes a splitting of the choline signal (point above 5 mM, same figure) as shown in Table 1. The addition of Mn^{2+} shows the disappearance of the peak corresponding to the signal of the choline

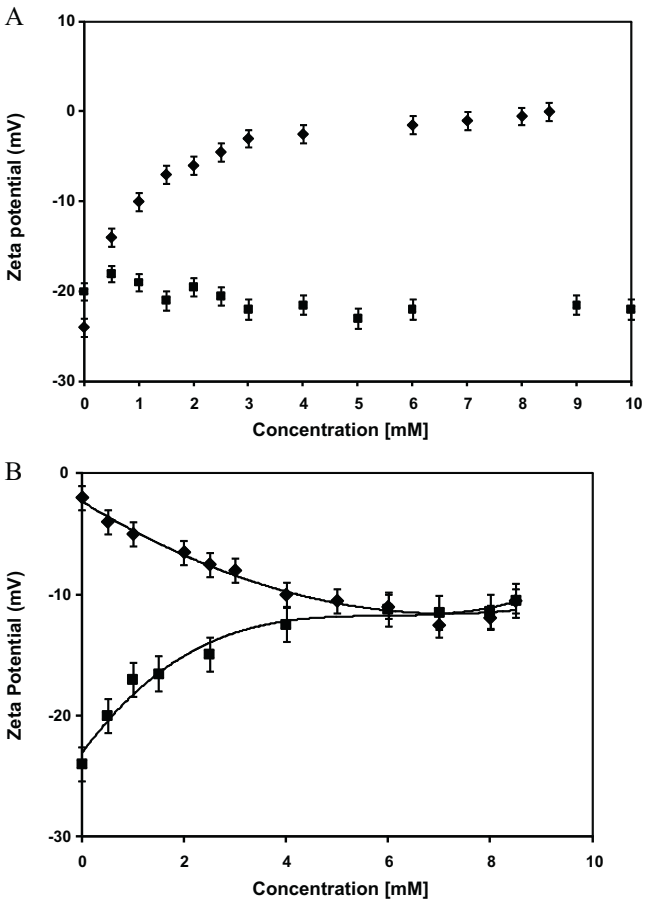

Fig. 5. Effect of Ca^{2+} and $[Fe(CN)_6]^{3-}$ on vesicle zeta potentials as measured by electrophoretic mobility. (A) Liposomes dispersed in water titrated with Ca^{2+} (■) and with ferricyanide (●) (B) $[Fe(CN)_6]^{3-}$ adsorption to bilayers saturated with Ca^{2+} (zeta potential zero as indicated in A upper curve) (■); Ca^{2+} adsorption to PC in the presence of $[Fe(CN)_6]^{3-}$ (zeta potential according to A lower curve) (●).

Table 1
^1H NMR signal shift of choline groups in the presence of Ca^{2+}, ferricyanide and Ca^{2+} + ferricyanide.

	External choline (ppm)	Internal choline (ppm)	Splitting (Hz)
Ca^{2+}	3.08	3.08	0
$K_3[Fe(CN)_6]$	3.07	3.07	0
$K_3[Fe(CN)_6] + Ca^{2+}$	3.08	3.04	11.33

groups on the external layer of the bilayer (data not shown). This indicates that the splitting is caused by a shift of the signal of the outer cholines to higher fields by the interaction with Ca^{2+} and $[Fe(CN)_6]^{3-}$. The addition of a high Na^+ concentration instead of Ca^{2+} does not affect this signal indicating that the splitting effect is not due to ionic strength. However, the splitting of the signal caused by ferricyanide/Ca^{2+} is reversed either by the addition of ascorbic acid, and by increasing Na^+ concentration (Fig. 6A and B and Table 1).

Ca^{2+} and ferricyanide binding obtained by electrophoresis can be corroborated by direct observation of the phosphate group stretching frequencies by ATR-FTIR spectroscopy. The frequency

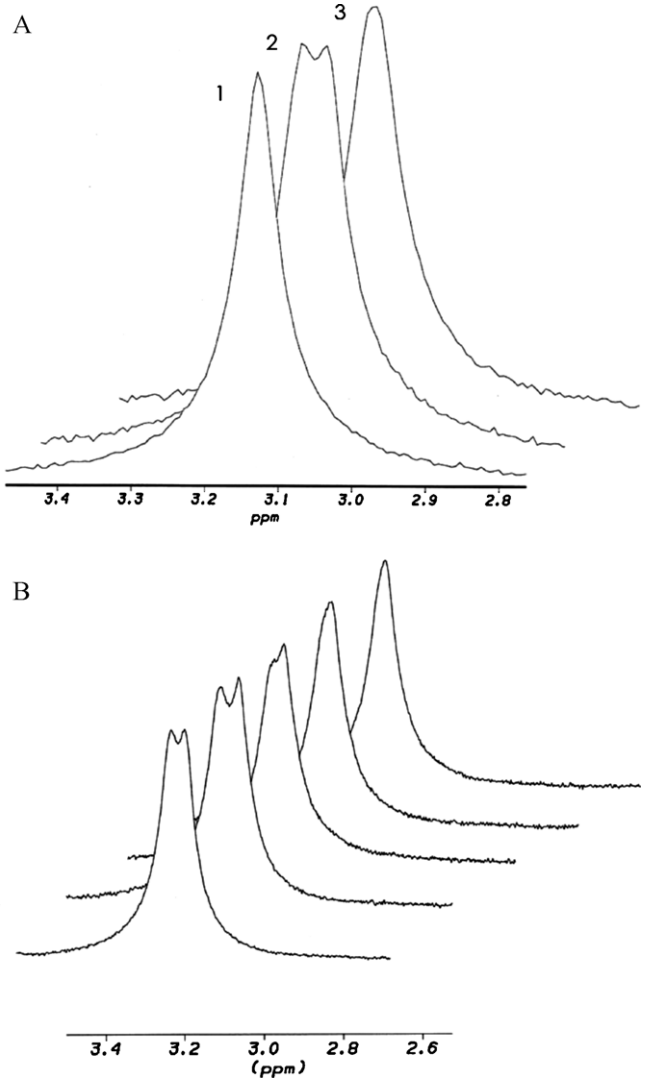

Fig. 6. Reversion of the splitting caused by the formation of the $Ca^{2+}/[Fe(CN)_6]^{3-}$ complex on lipid vesicles by (A) control (1); after addition of Ca^{2+} and ferricyanide (2); after addition of ascorbic acid to sample 2 (3). (B) Effect of increasing Na^+ on the signal splitting.

assigned to the asymmetric stretching of the PO group is usually taken as a measure of the hydration of the phosphate group. In Fig. 7 and Table 2, it is observed that Ca^{2+} shifts to higher values the frequencies corresponding to the asymmetric stretching bands indicating a partial dehydration. In the presence of ferricyanide, the asymmetric PO frequency decreases to that found with Ca^{2+} indicating a decrease of the PO bond strength as a consequence of the complex formation. The final value is still above for fully hydrated DPPC indicating that the nature of the Ca/ferricyanide interaction would be different than the H-bonds concerted by the PO with water molecules.

4. Discussion

Data of Fig. 5A show that Ca^{2+} adsorbs to membranes in contrast to $[Fe(CN)_6]^{3-}$. This conclusion is reached because the zeta potential shifts to positive values with Ca^{2+}, while the addition of ferricyanide alone does not change the negative zeta potential of the PC liposomes. This is corroborated by the observation that Ca^{2+} shifts the frequencies of the asymmetric phosphate stretching band but ferricyanide does not affect it. The fact that ferricyanide does not adsorb to PC membranes can be ascribed to the strong electrostatic repulsion between the anion (charge density = 0.0075) with the intrinsic negative charges of the surfaces, mainly the phosphate groups (charge density = 0.005). However, when these surface charges are neutralized at 5 mM Ca^{2+} (Fig. 5A upper curve), $[Fe(CN)_6]^{3-}$ adsorbs to the lipids when the potential of the surface is zeroed (Fig. 5B upper curve). These results indicate that $[Fe(CN)_6]^{3-}$ binds to vesicles by non-electrostatic forces. The adsorption can be explained by the high polarizability of this anion (53.3–50.7 $Å^3$ in comparison to 12 $Å^3$ of the ClO_4^-) [21]. This high polarizability can be ascribed to the deformability of the π orbitals of the CN^- ligands in ferricyanide. The deformability can be induced by the residual positive charge on the cholines and the residual positive charge of the Ca^{2+} ions bound to the phosphate groups. The high charge density = 0.02 and its very low polarizability (0.7–2 $Å^3$) makes Ca^{2+} an ion with a high polarizing strength.

In a lower magnitude, the charge density on the choline groups (density charge ca. 0.005) can also induce CN^- polarization and contribute to ferricyanide adsorption. This is sustained by the ^1H NMR data indicating that the choline groups are affected by $[Fe(CN)_6]^{3-}$ only in the presence of Ca^{2+}, i.e. when the surface potential is zero. The resonance of the inner and outer choline groups lies at the same values (3.08 ppm) as reported elsewhere [24] in the absence of the ions and the splitting is observed when Ca^{2+} and $[Fe(CN)_6]^{3-}$ are present, i.e. the conditions at which aggregation was observed.

The splitting of choline signal resonance has been previously reported in sonicated vesicles. The difference between the inner and the outer choline proton resonances of around 13 Hz being the inner choline shifted to higher fields was ascribed to the different head group conformation due to a higher packing of the phospholipids in the inner monolayer with respect to the outer one due to curvature [24]. In our case, when aggregates are formed in the presence of Ca^{2+} and $[Fe\ (CN)_6]^{3-}$, the splitting has a similar magnitude than that found in sonicated vesicles. However, it appears to be due to a shift of the outer choline signal to higher fields as denoted by the disappearance of the peak corresponding to the signal of the choline groups on the external layer of the bilayer due to the addition of Mn^{2+}. Thus, the formation of the complex at the outer surface promotes an increase in packing of the external phospholipids.

Thus, it may be concluded that the complex formation between opposing vesicles via the adsorption of $Ca^{2+}/[Fe(CN)_6]^{3-}$ complex promotes a tight structure decreasing the mobility of the choline groups in the outer face. These tight aggregates can be the reason of

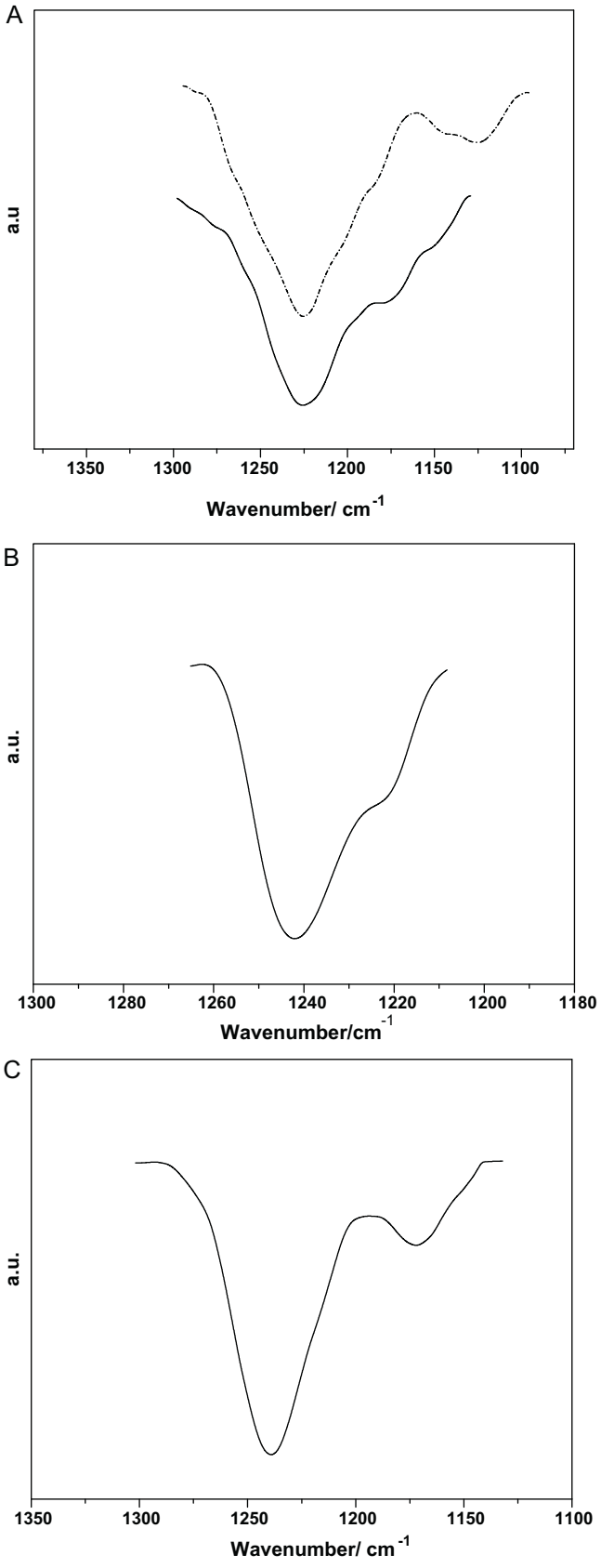

Fig. 7. FTIR spectra corresponding to phosphate asymmetric stretching bands. (A) DPPC in (dotted line) water or ferricyanide solution (full line). (B) DPPC in the presence of Ca^{2+}, C. DPPC in the presence of Ca^{2+} and ferricyanide. Ca^{2+}/ferricyanide ratios were the same as in Fig. 1.

Table 2
Frequency shift of the asymmetric stretching phosphate band of DPPC in the presence of Ca^{2+}, $K_3[Fe(CN)_6]$ and $K_3[Fe(CN)_6] + Ca^{2+}$.

	PC in H_2O or $K_3[Fe(CN)_6]$ solution	Standard deviation	DPPC in the presence of Ca^{2+}	Standard deviation	DPPC in the presence of $K_3[Fe(CN)_6] + Ca^{2+}$	Standard deviation	$\Delta\tilde{\nu}$ (cm^{-1})
PO_2^- antisym. (cm^{-1})	1230.6 1167.5	±0.2 ±0.6	1242.3 (11.7) 1221.4 (53.9)	±0.4 ±0.2	1238.8 (8.2) 1170.3 (2.8)	±0.2 ±0.1	−3.5 −51.1

Ratios of Ca^{2+} and ferricyanide with respect to lipids are the same as those in Fig. 1.
Values in parenthesis correspond to the difference in frequency with respect to pure DPPC in water at the same temperature (25 °C and RH% = 34).
$\Delta\nu$ values in the right hand column correspond to the difference between the frequencies of lipid in the presence of Ca^{2+} and those of lipid in Ca^{2+} plus ferricyanide.

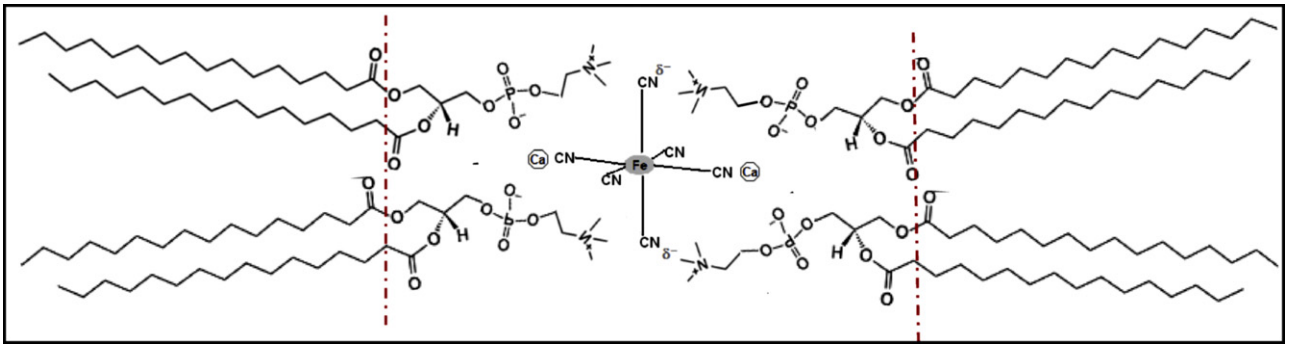

Fig. 8. Schematic model of the formation of a complex between opposing bilayers by the crosslinking of $Ca^{2+}/[Fe(CN)_6]^{3-}$.

the rough surfaces observed by electron microscopy in Fig. 2E. This may be explained because opposing vesicles attach each other via a bridge formed by the ferricyanide between Ca^{2+}/choline group of one vesicle and the Ca^{2+}/choline groups of the opposing one (Fig. 8).

The possibility that $[Fe(CN)_6]^{3-}$ adsorbs to the phosphatidylcholine and then Ca^{2+} forms bridges between opposing bilayers is unlikely since $[Fe(CN)_6]^{3-}$ does not adsorb to vesicles in the absence of Ca^{2+} as denoted by electrophoretic mobility and FTIR results (see Figs. 5 and 7). In contrast, ferricyanide added to a Ca^{2+}-lipid vesicle dispersion shifts the zeta potential from zero to negative values, concomitantly with a shift of the choline signal and of the frequency of the phosphate groups. This is also attained when Ca^{2+} and $[Fe(CN)_6]^{3-}$ are added simultaneously to the lipid dispersion. (Fig. 5, lower curve), denoting that Ca^{2+} adsorption is favoured both kinetically and energetically. This is consistent with the observation that Ca^{2+} promotes a partial dehydration of the phosphate region as a result of a strong Ca^{2+}–phosphate interaction (Table 2).

In this context it is worthy to recall that Ca^{2+} adsorbs [25] on phosphatidylcholine membranes in the gel phase with a 1:2 stoichiometry. That is, one Ca^{2+} is able to bind two adjacent phosphate groups. In addition, ^{31}P NMR results have shown that Ca^{2+} restricts the phosphate group mobility which is ascribed to partial dehydration [25]. The zeta potential equals to zero denoting that Ca^{2+} neutralizes the phosphate groups at 5–6 mM Ca^{2+}. The strong binding of Ca^{2+} to PO^- can be explained by a hard acid and hard bases interaction.

No net adsorption of $[Fe(CN)_6]^{3-}$ to phosphatidylcholines is apparent in the absence of Ca^{2+}. This conclusion can be inferred from the absence of changes in the zeta potential and in the phosphate stretching frequency measured by FTIR (Fig. 7A). However, adsorption occurs when the surface potential is zeroed by Ca^{2+}. In other words, the absence of repulsion forces, $[Fe(CN)_6]^{3-}$ binds to the membrane by different forces beside electrostatics. The shift to lower values of the asymmetric stretching band when the aggregation take place in the presence of Ca and ferricyanide with respect with the frequency observed with DPPC with Ca^{2+} (Table 2) indicates the formation of bonds of the PO group with the ion complex.

The alkyl groups at the choline are moderately hard bases due to the electronegativity of the N donor atom. This may contribute to the interaction of the cyanide of the ferricyanide because CN^- softens the hard acid of the Fe^{3+}.

The puzzle is why ferrocyanide, being so similar to ferricyanide, does not cause aggregation. As ferricyanide is the only anion able to induce aggregation, since neither ferrocyanide nor any other of the highly polarizable ions in the Hoffmeister series produces it, it is likely that ferricyanide fits special conditions in relation to ferrocyanide.

The previous observations indicating that the effect of $Ca^{2+}/[Fe(CN)_6]^{3-}$ is reversed by ascorbic acid, as visualized by the disappearance of the aggregation and the splitting, which induces the conversion of $[Fe(CN)_6]^{3-}$ to $[Fe(CN)_6]^{4-}$ is again a strong indication that the electrostatic charges are not the reason for aggregation [22]. The external radius of the ferrocyanide (450 nm) is larger than the ferricyanide (400 nm) due to the lower density charge of the Fe^{2+} in comparison to Fe^{3+}. This may be a steric hindrance for the formation of the complex. Thus, it is likely that the contact between opposing surfaces with Ca^{2+} fits well with the distance between CN^- in ferricyanide but not in ferrocyanide.

All together, these results suggest that $[Fe(CN)_6]^{3-}$ fits to form a complex between two opposing phospholipid monolayers of adjacent vesicles by non electrostatic forces.

In conditions in which Ca^{2+} is bound to the phosphate groups of two adjacent phosphocholines (see Fig. 8), $[Fe(CN)_6]^{3-}$ can bind by approaching one CN^- ligand to Ca^{2+} and the other two to the cholines. Cyanide π orbitals can be polarized by the high density charge of Ca^{2+} ions.

In consequence, these results provide evidence that aggregation of lipid vesicles may be a consequence of the formation of a supramolecular complex which is dominated by the oxidation state of the central nucleus such as Fe^{+3}. Further studies in this regard should demonstrate if other ligands to Fe^{3+} or similar complex with other central ions can form the same vesicle aggregates.

The properties of the aggregation–disaggregation by the redox potential can be an important tool to modulate the penetration-delivery of encapsulated compounds in lipid vesicles.

References

[1] V.A. Parsegian, N. Fuller, R.P. Rand, PNAS 76 (1979) 2750–2754.
[2] R.P. Rand, V.A. Parsegian, Biochimica et Biophysica Acta (BBA) 988 (1989) 351–376.
[3] T.J. McIntosh, Current Opinion in Structural Biology 10 (2000) 481–485.
[4] E.R. Lamberson, R. Cambrea Lee, J.S. Hovis, The Journal of Physical Chemistry B, Letters 111 (2007) 13664–13667.
[5] R. Pedersen, U. Leidy, C. Westh, P.G.H. Peters, Biochimica et Biophysica Acta (BBA)–Biomembranes 1758 (5) (2006) 573–582.
[6] R.D. Porasso, J.J. López Cascales, Colloids and Surfaces B: Biointerfaces 73 (2009) 42–50.
[7] L. Ilya, D.A. Christian, Y.-H. Wang, J.J. Madara, Discher, E. Dennis, Janmey, A. Paul, Biochemistry 48 (34) (2009) 8241–8248.
[8] R. Lee, F. Haque, J.L. Schieler, J.-C. Rochet, J.S. Hovis, Biophysical Journal 93 (2007) 1630–1638.
[9] H. Hauser, R.M.C. Dawson, European Journal of Biochemistry 1 (1967) 61–69.
[10] K. Satoh, Biochimica et Biophysica Acta 1239 (1995) 239–248.
[11] C.R. Flach, J.W. Brauner, R. Mendelsohn, Biophysical Journal 65 (1993) 1994–2001.
[12] J. Grdadonik, D. Hadzi, Chemistry and Physics of Lipids 65 (1993) 121–132.
[13] W. Pohle, M. Bohl, H. Bohlig, Journal of Molecular Structure 242 (1991) 333–342.
[14] E.M. Goldberg, D.S. Lester, D.B. Borchardt, R. Zidovetzki, Biophysical Journal 66 (1994) 382–393.
[15] E.A. Disalvo, L.S. Bakas, Bioelectrochemistry and Bioenergetics 20 (1988) 257–267.
[16] C. Faure, L. Bonakdar, E.J. Dufourc, FEBS Letters 405 (1997) 263–266.
[17] A.L.Y. Lau, A.C. McLaughlin, R.C. MacDonald, S.G.A. Mc Laughlin, in: M. Blank (Ed.), Advances in Chemistry Series, vol. 188, Am. Chem. Soc., Washington, DC, 1980, pp. 49–56 (Chapter 3).
[18] S.A. Tatulian, European Journal of Biochemistry 170 (1987) 413–420.
[19] J.R. Rydall, P.M. Macdonald, Biochemistry 31 (1992) 1092–1099.
[20] J. Lyklema, Chemical Physics Letters 467 (2009) 217–222.
[21] Y. Marcus, Ion Properties, first ed., Marcel Dekker, New York, 1997.
[22] L.S. Bakas, E.A. Disalvo, Biochimica et Biophysica Acta (BBA)–Biomembranes 939 (2) (1988) 295–304.
[23] A.D. Bangham, M.M. Standish, J.C. Watkins, Journal of Molecular Biology 13 (1965) 238–252.
[24] K.E. Eisenberg, S.I. Chan, Biochimica et Biophysica Acta 599 (1980) 330–335.
[25] L.J. Lis, W.T. Lis, V.A. Parsegian, R.P. Rand, Biochemistry 20 (1981) 1771–1777.